Hydrothermal syntheses, structural characterization, and photoluminescent properties of five lanthanide coordination polymers

Guangbo Che [a] [b] , Xiangcheng Wang [b] , Chunbo Liu [a] [b] , Jing Chen [b] , Shanshan Wang [a] & Xiuying Li [a]

[a] Key Laboratory of Preparation and Applications of Environmental Friendly Materials , Jilin Normal University, Chinese Ministry of Education , Siping 136000 , People's Republic of China
[b] School of Chemistry and Chemical Engineering, Jiangsu University , Zhenjiang 212013 , People's Republic of China
Accepted author version posted online: 05 Oct 2012.Published online: 22 Oct 2012.

PLEASE SCROLL DOWN FOR ARTICLE

Hydrothermal syntheses, structural characterization, and photoluminescent properties of five lanthanide coordination polymers

GUANGBO CHE*†‡, XIANGCHENG WANG‡, CHUNBO LIU†‡,
JING CHEN‡, SHANSHAN WANG† and XIUYING LI†

†Key Laboratory of Preparation and Applications of Environmental Friendly Materials,
Jilin Normal University, Chinese Ministry of Education, Siping 136000,
People's Republic of China
‡School of Chemistry and Chemical Engineering, Jiangsu University, Zhenjiang 212013,
People's Republic of China

Five mixed-ligand coordination polymers, $[Ln_2(PTCP)_2(m\text{-}BDC)_3]_n \cdot nH_2O$ (Ln = Pr (**1**), Sm (**2**), Eu (**3**), Tb (**4**), Dy (**5**); m-BDC = 1,3-benzenedicarboxylate; PTCP = 2-phenyl-1H-1,3,7,8-tetraazacyclopenta[l]phenanthrene), were synthesized and characterized by IR spectra, elemental analyses, thermogravimetric analyses, single-crystal X-ray diffraction, and solid-state photoluminescent spectra. X-ray crystallographic analyses reveal that the five complexes are 1-D structures based on dinuclear $[Ln_2O_{12}N_4]$ units and further assembled into 3-D supramolecular networks by hydrogen bonds and $\pi \cdots \pi$ stacking interactions. The solids possess high thermal stabilities, with **3** and **4** exhibiting strong pure red and green characteristic emissions of Eu(III) and Tb(III) at room temperature.

Keywords: Hydrothermal; Lanthanide; 1,3-Benzenedicarboxylate; 2-Phenyl-1H-1,3,7,8-tetraazacyclopenta[l]phenanthrene; Photoluminescence

1. Introduction

Metal coordination polymers with N-containing ligands have attracted attention for fascinating structures [1] and potential applications in gas adsorption, magnetism, heterogeneous catalysis, luminescence, and nonlinear optics [2–6]. 1,10-Phenanthrene and derivatives possess large π-conjugated plane and attractive coordination abilities which are extensively used in synthesis of solid materials [7]. The $\pi \cdots \pi$ stacking interaction of aromatic rings plays a significant role in assembly of high-dimensional networks [8]. 2-Phenyl-1H-1,3,7,8-tetraazacyclopenta[l]phenanthrene (PTCP) contains five condensation rings and four nitrogen atoms, two being donors at the phenanthroline moiety and two nitrogen atoms from the imidazole portion [9]. The site is a π-acceptor and is also suited for H-bonding with H-donors.

---

*Corresponding author. Email: guangbochejl@yahoo.com

Various aromatic multicarboxylates have been referred to as secondary building units in the construction of metal–organic frameworks (MOFs) because of rigidity unlikely to deform during assembly [10] and abilities to aggregate metal ions into MOFs clusters [11]. Generally, carboxylates adopt various binding modes, terminal monodentate, monodentate bridging, chelating bidentate to one metal center, bridging bidentate in syn–syn, syn–anti, and anti–anti fashions to two metal centers, and chelating-bridging tridentate to two metal centers [12].

Aromatic carboxylates that directly link lanthanides are studied for unique optical properties such as long-lived luminescence lifetimes, narrow-band emission peaks, and unpolarized luminescence [13]. These characteristics are important to solid-state lasers, optical communication amplifiers, and screens. Lanthanide coordination polymers based on PTCP have rarely been investigated [14].

In our work, PTCP and 1,3-benzenedicarboxylic acid (m-H_2BDC) react with lanthanide salts. We report five new carboxylates, [Ln_2(PTCP)$_2$(m-BDC)$_3$]$_n \cdot n H_2O$ (Ln = Pr (**1**), Sm (**2**), Eu (**3**), Tb (**4**), Dy (**5**)). The polymers are 1-D chains and further assemble into 3-D supramolecular networks *via* hydrogen bonds and $\pi \cdots \pi$ stacking interactions between the ligands. Complexes **3** and **4** exhibit strong pure red and green emissions of Eu(III) and Tb(III) in the solid state at room temperature.

2. Experimental

2.1. *General*

Pr_6O_{11}, Tb_4O_7, Ln_2O_3 (Ln = Sm, Eu, Dy), and m-H_2BDC were commercially obtained and used without purification. PTCP was prepared according to reported procedures [15]. IR spectra were recorded as KBr pellets on a Bruker IFS 66 V/S FTIR spectrometer from 4000 to 400 cm^{-1}. Elemental analyses were performed on a Perkin-Elmer 240 analyzer. Thermogravimetric analysis (TGA) was performed on a TA Instrument with a heating rate of 10°C min^{-1} under air. Solid-state luminescence spectroscopy was performed on a Perkin-Elmer LS55 spectrometer.

2.2. *Synthesis of 1*

A mixture of PTCP (0.3 mmol), m-H_2BDC (0.3 mmol), Pr_6O_{11} (0.033 mmol), NaOH (0.4 mmol), and H_2O (15 mL) was placed in a Teflon-lined stainless steel vessel (25 mL), heated at 160°C for 72 h and then cooled to room temperature at a rate of 5°C h^{-1}. The resulting yellow crystalline **1** was obtained, washed with H_2O, and dried in air (yield 29% based on Pr). Anal. Calcd for $C_{62}H_{36}Pr_2N_8O_{13}$: C, 53.72; H, 2.74; N, 8.09. Found: C, 53.58; H, 2.70; N, 8.14. IR (KBr, cm^{-1}): 3069.89 m(ν(N–H)), 1608.39 s(ν_s(COO–)), 1544.61 s(ν(C=N)), 1478.86 s(ν_{as}(COO–)), 1394.25 s(ν(C=C)), 1388.30 s(ν(C=N)), 813.96 m(δ(C–H)), 741.34 m(ν(Pr–N)), 556.83 w(ν(Pr–N)), 416.07 m(ν(Pr–O)).

2.3. *Synthesis of 2*

An identical procedure with **1** was followed to prepare **2** except Pr_6O_{11} was replaced by Sm_2O_3 (0.1 mmol). Pale yellow cubic crystals of **2** formed in 82% yield (based on Sm).

Anal. Calcd for $C_{62}H_{36}Sm_2N_8O_{13}$: C, 53.00; H, 2.71; N, 7.98. Found: C, 53.06; H, 2.72; N, 8.02. IR (KBr, cm^{-1}): 3060.47 m(ν(N–H)), 1602.91 m(ν_s(COO–)), 1562.18 s(ν(C=N)), 1456.30 s(ν_{as}(COO–)), 1396.84 s(ν(C=C)), 1351.29 s(ν(C=N)), 805.60 m(δ(C–H)), 739.94 s(ν(Sm–N)), 514.93 w(ν(Sm–N)), 424.31 m(ν(Sm–O)).

2.4. Synthesis of 3

An identical procedure with **1** was followed to prepare **3** except Pr_6O_{11} was replaced by Eu_2O_3 (0.1 mmol). Pale yellow cubic crystals of **3** formed in 75% yield (based on Eu). Anal. Calcd for $C_{62}H_{36}Eu_2N_8O_{13}$: C, 52.91; H, 2.70; N, 7.96. Found: C, 52.97; H, 2.72; N, 7.95. IR (KBr, cm^{-1}): 3072.94 m(ν(N–H)), 1637.14 s(ν_s(COO–)), 1543.21 s(ν(C=N)), 1451.40 s(ν_{as}(COO–)), 1400.41 s(ν(C=C)), 1278.17 m(ν(C=N)), 814.04 w(δ(C–H)), 743.13 m(ν(Eu–N)), 544.27 w(ν(Eu–N)), 418.56 m(ν(Eu–O)).

2.5. Synthesis of 4

An identical procedure with **1** was followed to prepare **4** except Pr_6O_{11} was replaced by Tb_4O_7 (0.05 mmol). Pale yellow cubic crystals of **4** formed in 31% yield (based on Tb). Anal. Calcd for $C_{62}H_{36}Tb_2N_8O_{13}$: C, 52.39; H, 2.67; N, 7.87. Found: C, 52.53; H, 2.70; N, 7.84. IR (KBr, cm^{-1}): 3074.23 m(ν(N–H)), 1629.46 s(ν_s(COO–)), 1539.48 s(ν(C=N)), 1448.60 s(ν_{as}(COO–)), 1394.25 s(ν(C=C)), 818.08 w(δ(C–H)), 745.41 m(ν(Tb–N)), 529.80 w(ν(Tb–N)), 424.70 m(ν(Tb–O)).

2.6. Synthesis of 5

An identical procedure with **1** was followed to prepare **5** except Pr_6O_{11} was replaced by Dy_2O_3 (0.1 mmol). Pale yellow cubic crystals of **5** formed in 72% yield (based on Dy). Anal. Calcd for $C_{62}H_{36}Dy_2N_8O_{13}$: C, 52.13; H, 2.66; N, 7.85. Found: C, 52.23; H, 2.70; N, 7.88. IR (KBr, cm^{-1}): 3070.33 m(ν(N–H)), 1645.86 s(ν_s(COO–)), 1554.83 s(ν(C=N)), 1452.70 s(ν_{as}(COO–)), 1408.52 s(ν(C=C)), 813.63 w(δ(C–H)), 749.18 s(ν(Dy–N)), 534.13 m(ν(Dy–N)), 424.19 m(ν(Dy–O)).

2.7. Single-crystal X-ray diffraction

Single-crystal X-ray data were collected at room temperature on an Oxford Diffraction Gemini R Ultra diffractometer equipped with graphite monochromated Mo-Kα radiation ($\lambda = 0.71073$ Å) at 292(2) K by using a ω-scan mode. The structure was solved by direct methods and refined by full-matrix least-squares based on F^2 using SHELXS-97 and SHELXTL-97 [16]. All non-hydrogen atoms were refined anisotropically and hydrogen atoms of organic ligands were generated geometrically. Free water molecules in **1**–**5** are disordered and the hydrogen atoms are not found in the electron density map. The crystallographic data of **1**–**5** are summarized in table 1 and selected bond distances in table 2.

Table 1. Crystallographic data for **1**–**5**.

	1	2	3	4	5
Formula	$C_{62}H_{36}Pr_2N_8O_{13}$	$C_{62}H_{36}Sm_2N_8O_{13}$	$C_{62}H_{36}Eu_2N_8O_{13}$	$C_{62}H_{36}Tb_2N_8O_{13}$	$C_{62}H_{36}Dy_2N_8O_{13}$
Formula weight	1382.81	1401.69	1404.93	1418.83	1428.00
Crystal system	Monoclinic	Monoclinic	Monoclinic	Monoclinic	Monoclinic
Space group	$P\,21/m$	$P\,21/m$	$P\,21/m$	$P\,21/m$	$P\,21/m$
Unit cell dimensions (Å, °)					
a	9.855(3)	9.8248(4)	9.830(4)	9.8355(4)	9.828(2)
b	18.435(5)	18.2635(5)	18.206(8)	18.0856(5)	18.047(4)
c	15.636(4)	15.6135(6)	15.592(7)	15.6259(6)	15.591(3)
β	102.333(3)	101.820(4)	101.722(5)	101.052(4)	101.07
Volume (Å³), Z	2775.1(13), 2	2742.21(17), 2	2363.2 (2), 2	2728.00(17), 2	2713.8(9), 2
Calculated density (Mg m⁻³)	1.655	1.698	1.708	1.727	1.748
Crystal size (mm³)	$0.33 \times 0.25 \times 0.18$	$0.30 \times 0.22 \times 0.14$	$0.29 \times 0.24 \times 0.14$	$0.53 \times 0.44 \times 0.40$	$0.47 \times 0.38 \times 0.34$
$F(000)$	1372	1384	1388.0	1396	1404
Absorption coefficient (mm⁻¹)	1.810	2.196	2.351	2.648	2.747
θ range for data collection (°)	2.21–26.08	4.32–29.28	2.12–26.11	2.89–29.01	3.06–27.47
Limiting indices	$-12 \le h \le 12;$	$-8 \le h \le 13;$	$-12 \le h \le 12;$	$-12 \le h \le 12;$	$-12 \le h \le 12;$
	$-22 \le k \le 22;$	$-24 \le k \le 19;$	$-22 \le k \le 22;$	$-23 \le k \le 16;$	$-22 \le k \le 22;$
	$-18 \le l \le 19$	$-19 \le l \le 20$	$-19 \le l \le 19$	$-15 \le l \le 21$	$-18 \le l \le 19$
Reflections collected/unique	23,938/5666	13,578/6625	23,537/5582	12,139/6347	23,938/5666
Goodness-of-fit on F^2	1.022	1.036	1.048	0.946	1.079
Final R indices [$I > 2\sigma(I)$]	$R_1 = 0.0432,$	$R_1 = 0.0468,$	$R_1 = 0.0496,$	$R_1 = 0.0445,$	$R_1 = 0.0529,$
	$wR_2 = 0.1108$	$wR_2 = 0.0941$	$wR_2 = 0.1228$	$wR_2 = 0.0650$	$wR_2 = 0.1503$
R indices (all data)	$R_1 = 0.0481,$	$R_1 = 0.0858,$	$R_1 = 0.0666,$	$R_1 = 0.0952,$	$R_1 = 0.0579,$
	$wR_2 = 0.1145$	$wR_2 = 0.0992$	$wR_2 = 0.1337$	$wR_2 = 0.0680$	$wR_2 = 0.1551$

Table 2. Selected bond distances (Å) for **1–5**.

1

Pr–N(1)	2.630(4)	Pr–N(2)	2.672(4)	Pr–O(1)	2.785(4)
Pr–O(2)	2.390(4)	Pr–O(3)	2.457(4)	Pr–O(4)	2.383(4)
Pr–O(5)	2.452(3)	Pr–O(6)	2.414(3)		

2

Sm–N(1)	2.621(5)	Sm–N(2)	2.581(5)	Sm–O(1)	2.347(4)
Sm–O(2)	2.775(4)	Sm–O(3)	2.402(4)	Sm–O(4)	2.364(4)
Sm–O(5)	2.418(4)	Sm–O(6)#1	2.327(4)		

3

Eu–N(1)	2.558(4)	Eu–N(2)	2.611(4)	Eu–O(1)	2.324(3)
Eu–O(2)	2.775(4)	Eu–O(3)#2	2.354(3)	Eu–O(4)	2.379(3)
Eu–O(5)	2.394(3)	Eu–O(6)#2	2.315(4)		

4

Tb–N(1)	2.580(5)	Tb–N(2)	2.539(5)	Tb–O(1)	2.294(4)
Tb–O(2)	2.752(5)	Tb–O(3)	2.327(4)	Tb–O(4)#3	2.348(4)
Tb–O(5)	2.366(4)	Tb–O(6)	2.282(4)		

5

Dy–N(1)	2.632(5)	Dy–N(2)	2.674(5)	Dy–O(1)	2.786(4)
Dy–O(2)	2.390(4)	Dy–O(3)	2.455(4)	Dy–O(4)	2.384(5)
Dy–O(5)	2.449(4)	Dy–O(6)	2.413(4)		

Symmetry transformations used to generate equivalent atoms in **1–5**: #1: $-x, -y, -z+1$; #2: $-x+1, -y, -z$; #3: $-x+1, -y, -z+2$.

3. Results and discussion

3.1. *Description of crystal structure*

X-ray crystallographic study revealed that **1–5** are isostructural, so **3** represents **1–5** for detailed structural description. As shown in Supplementary material, Eu and EuA in the dinuclear species are both eight-coordinate by two nitrogen atoms from one chelated PTCP and six oxygen atoms from five m-BDC in which four μ-O_2C oxygen atoms are from four m-BDC ligands and two chelated O_{COO}^- are from another m-BDC. Eu–O bond lengths are 2.315(4)–2.775(4) Å and Eu–N bond lengths are 2.611(4) Å (Eu–N2) and 2.558(4) Å (Eu–N1). The Eu⋯EuA distance in the dinuclear units [$Eu_2O_{12}N_4$] is 4.0961(18) Å. Complex **3** is a 1-D chain structure linked by m-BDC and decorated by PTCP. The dinuclear units [$Eu_2O_{12}N_4$] are bridged by three m-BDC ligands forming a three-strand chain structure and m-BDC are arranged in wave shape which can be seen more clearly in the space-filling diagram (figure 1a). Then PTCP ligands are decorated at both sides of the three-strand chain like a zipper (figure 1b). The m-BDC ligands hold two different coordination modes and all oxygen atoms take part in coordination to the two rare-earth ions: (1) chelating bidentate, two carboxylates from m-BDC anions chelate two Eu in neighboring units as a bridge (scheme 1a) and (2) syn–syn bridging bidentate (scheme 1b). The coordination mode of m-BDC in **3** is different from [Zn(m-bdc)(bth)]$_n$ [17] and {[Zn(btp)(1,3-bdc)(H$_2$O)]·1.5H$_2$O}$_n$ [18].

In **3**, m-BDC and PTCP in neighboring chains give $\pi \cdots \pi$ stacking interactions including face-to-face and edge-to-face, shown in figure 2. The centroid-to-centroid distances of the multipoint face-to-face $\pi \cdots \pi$ interactions between PTCP are about 3.70 Å and the shortest atom-to-centroid distances of 3.50 Å. There is a weak
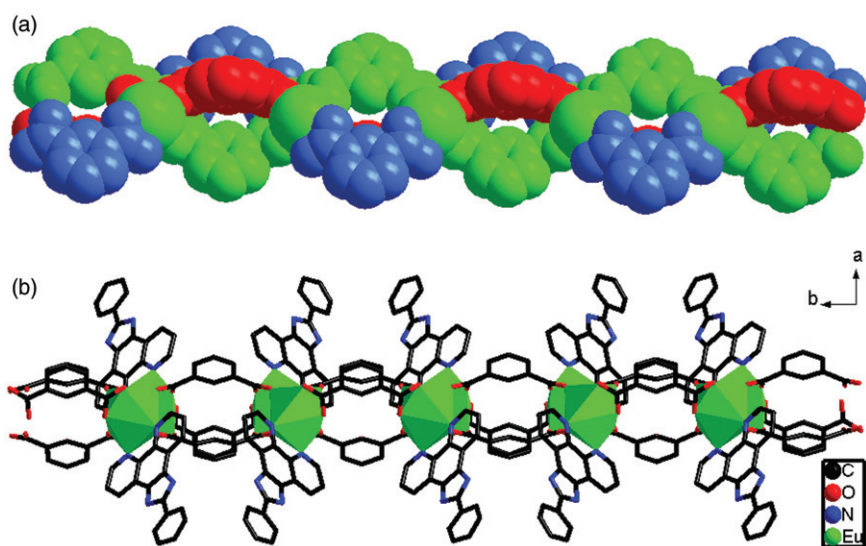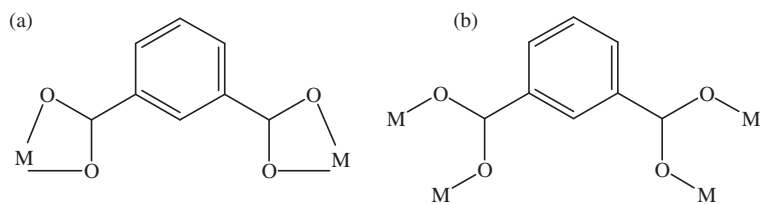
Figure 1.   (a) View of a three-strand chain in space-filling diagram and (b) view of the 1-D zipper-like chain through the Eu–O interaction for **3**; the polyhedra show the [EuO$_6$N$_2$] units.

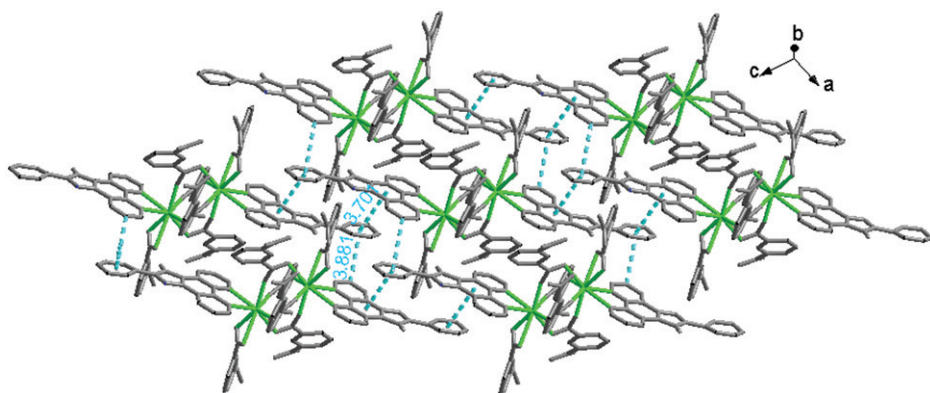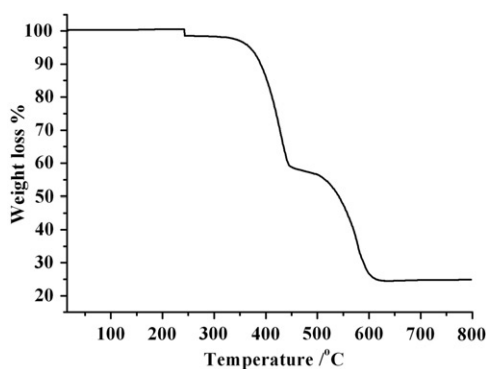Scheme 1.   Coordination modes of m-BDC ligands in **1**–**5**.

Figure 2. $\pi \cdots \pi$ stacking interactions between PTCP ligands in **3**.

Figure 3. TG analysis of **3**.

edge-to-face $\pi \cdots \pi$ interaction between PTCP ligands with the atom-to-centroid distances of 3.88 Å and the nearest carbon distances of 3.57 Å (C2$\cdots$C19). A strong N–H$\cdots$O hydrogen bond is observed between imidazole N4–H of PTCP and O2 of carboxylate (N–H = 0.8600(2), N$\cdots$O = 2.828(26) Å, hydrogen-bonds angles = 166.23(2)°). Those non-covalent bonds in **3** result in a 3-D supramolecular network shown in Supplementary material.

3.2. Thermogravimetric analyses

TGA was performed to determine the stabilities of **1**–**5**. Owing to the structural similarity of **1**–**5**, **3** was selected with TG results showing that **3** is stable in air and the first weight loss of 1.4% (Calcd 1.3%) corresponds to removal of the non-coordinated water at 240°C. From 240°C to 350°C, **3** shows good stability. The second weight loss of 41.8 (Calcd 42.5%) between 350°C and 450°C is attributed to the loss of PTCP. The third weight loss from 450°C and 610°C corresponds to decomposition of m-BDC (observed 31.9%; expected 31.0%) (figure 3).

3.3. Photoluminescence

Rare-earth cations produce a variety of complexes that possess photoluminescence (PL) properties. The luminescent properties of **1**–**5** in the solid state at room temperature were investigated. The PL spectra of **3** and **4** at room temperature are depicted in figure 4(a) and (b). Luminescent spectra of **3** and **4** were measured upon excitation at 375 nm; luminescent properties of **1**, **2**, and **5** were not made because luminescences of Pr(III), Sm(III), Dy(III) are less efficient. To understand the nature of these emission bands, the PL properties of PTCP and m-H$_2$BDC were also analyzed, showing they exhibit strongest emission at 475 nm [19] and 380 nm [20], respectively. Emission spectra of **3** and **4** are different than free ligands, attributed to characteristic emission bands of rare-earth ions. Complex **3** has the most intense emission at 618 nm corresponding to $^5D_0 \rightarrow {}^7F_2$ transition of Eu(III). The five peaks in figure 4(a) correspond to $^5D_0 \rightarrow {}^7F_1$, $^5D_0 \rightarrow {}^7F_2$, $^5D_0 \rightarrow {}^7F_3$, and $^5D_0 \rightarrow {}^7F_4$ transitions of Eu(III), respectively. Complex **4**
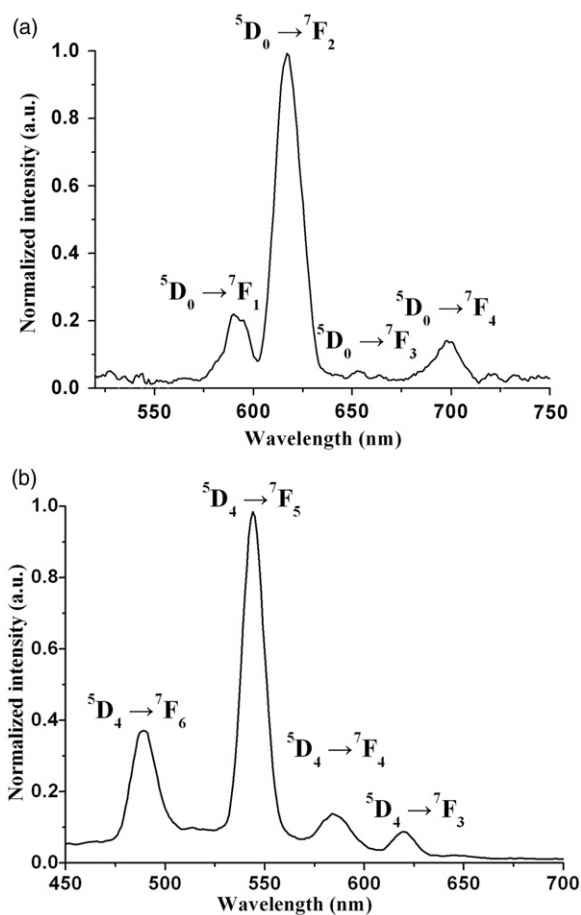
Figure 4. (a) The emission spectrum of **3** in solid state, excited at 375 nm and (b) the emission spectrum of **4** in solid state, excited at 375 nm.

has intense and pure green luminescence (figure 4b). Four peaks at 490, 544, 650, and 620 nm are assigned to the transition of Tb(III) from $^5D_4 \rightarrow {}^7F_J$ ($J = 6$, 5, 4, and 3).

4. Conclusion

Lanthanide complexes based on PTCP ligand, $[Ln_2(PTCP)_2(m\text{-}BDC)_3]_n \cdot nH_2O$ (Ln = Pr (**1**), Sm (**2**), Eu (**3**), Tb (**4**), Dy (**5**)), have been obtained by hydrothermal synthesis and characterized by single-crystal X-ray diffraction. The results show that m-BDC is a bridging ligand linking the dinuclear inorganic units $[Ln_2O_{12}N_4]$, leading to a strand-like structure and PTCP decorates at both sides of the strand forming a zipper-like structure. The 1-D chains are assembled into a 3-D supermolecular network *via* $\pi\cdots\pi$ stacking interactions and hydrogen bonds. Coordination polymers **3** and **4** emit strong luminescence of Eu(III) and Tb(III) in the solid state at room temperature.

Supplementary material

Crystallographic data for $[Ln_2(PTCP)_2 (m\text{-}BDC)_3]_n \cdot nH_2O$ (Ln = Pr (**1**), Sm (**2**), Eu (**3**), Tb (**4**), Dy (**5**)) have been deposited with the Cambridge Crystallographic Data Center as supplementary publications CCDC 782264, 783272, 782262, 782263, and 782 264. Copies of the data can be obtained free of charge on application to CCDC, 12 Union Road, Cambridge CB2 1EZ, UK; Fax (+44) 1 223 336 033; E-mail: deposit@ccdc.cam.ac.uk.

Acknowledgments

References

[1] (a) A.Y. Robin, K.M. Fromm. *Coord. Chem. Rev.*, **250**, 2127 (2006); (b) G.B. Che, C.B. Liu, B. Liu, Q.W. Wang, Z.L. Xu. *CrystEngComm*, **10**, 184 (2008).

[2] (a) K.S. Park, Z. Ni, A.P. Côté, J.Y. Choi, R. Huang, F.J. Uribe-Romo, H.K. Chae, M. O'Keeffe, O.M. Yaghi. *PNAS*, **103**, 10186 (2006); (b) H. Li, A. Laine, M. O'Keeffe, O.M. Yaghi. *Science*, **283**, 1445 (1999).

[3] (a) P. Mahata, S. Natarajan, P. Panissod, M. Drillon. *J. Am. Chem. Soc.*, **131**, 10140 (2009); (b) B.Q. Ma, S. Gao, G. Su, G.X. Xu. *Angew. Chem. Int. Ed.*, **40**, 434 (2001).

[4] (a) C.D. Wu, A. Hu, L. Zhang, W.B. Lin. *J. Am. Chem. Soc.*, **127**, 8940 (2005); (b) J.H. Bi, L.T. Kong, Z.X. Huang, J.H. Liu. *Inorg. Chem.*, **47**, 4564 (2008).

[5] (a) M.D. Allendorf, C.A. Bauer, R.K. Bhaktaa, R.J.T. Houk. *Chem. Soc. Rev.*, **38**, 1330 (2009); (b) H. Jude, J.A.K. Bauer, W.B. Connick. *Inorg. Chem.*, **44**, 1211 (2005).

[6] O.R. Evans, W.B. Lin. *Acc. Chem. Res.*, **35**, 511 (2005).

[7] (a) G.B. Che, J. Wang, C.B. Liu, X.Y. Li, B. Liu, J. Sun, Y. Liu, L. Lu. *Inorg. Chim. Acta*, **362**, 2756 (2009); (b) J.R. Nitschke, D. Schultz, G. Bernardinelli, D. Gérard. *J. Am. Chem. Soc.*, **125**, 16538 (2004); (c) W.W. Brandt, F.P. Dwyer, E.D. Gyarfas. *Chem. Rev.*, **54**, 959 (1954); (d) X.Y. Li, C.B. Liu, G.B. Che, X.C. Wang, C.X. Li, Y.S. Yan, Q.F. Guan. *Inorg. Chim. Acta*, **363**, 1359 (2010).

[8] B.H. Ye, M.L. Tong, X.M. Chen. *Coord. Chem. Rev.*, **249**, 545 (2005).

[9] Q. Han, X.C. Wang, X.Y. Li, G.X. Yao, Y.S. Yan. *Acta Cryst. E*, **65**, m1282 (2009).

[10] H.M. El-Kaderi, J.R. Hunt, J.L. Mendoza-Cortés, A.P. Côté, R.E. Taylor, M. O'Keeffe, O.M. Yaghi. *Science*, **316**, 268 (2007).

[11] M. Eddaoudi, D.B. Moler, H. Li, B. Chen, T.M. Reineke, M. O'Keeffe, O.M. Yaghi. *Acc. Chem. Res.*, **34**, 4 (2001).

[12] (a) D.X. Hu, F. Luo, Y.X. Che, J.M. Zheng. *Cryst. Growth Des.*, **7**, 1733 (2007); (b) L.P. Zhang, Y.H. Wan, L.P. Jin. *Polyhedron*, **22**, 981 (2003); (c) G.X. Liu, R.Y. Huang, H. Xu, X.J. Kong, L.F. Huang, K. Zhu, X.M. Ren. *Polyhedron*, **27**, 2327 (2008).

[13] (a) J.C.G. Bünzli, C. Piguet. *Chem. Soc. Rev.*, **34**, 1048 (2005); (b) Y.L Qu, Y.X. Ke, S.M. Lu, R. Fan, G.Q. Pan, J.M. Li. *J. Mol. Struct.*, **734**, 7 (2005); (c) H.T. Xu, Y.D. Li. *J. Mol. Struct.*, **690**, 137 (2004).

[14] X.C. Wang, C.B. Liu, J. Chen, X.Y. Li, G.B. Che, Y.S. Yan. *Z. Anorg. Allg. Chem.*, **637**, 698 (2011).

[15] (a) A.D. Bettencourt-Dias, *Inorg. Chem.*, **44**, 2734 (2005); (b) S. Bodige, F.M. MacDonnell. *Tetrahedron Lett.*, **38**, 8159 (1997).

[16] (a) G.M. Sheldrick. *SHELXS 97, Program for the Solution of Crystal Structure*, University of Göttingen, Germany (1997); (b) G.M. Sheldrick. *SHELXTL97, Program for Crystal Structure Refinement*, University of Göttingen, Germany (1997).

[17] P. Zhang, D.-S. Li, J. Zhao, Y.-P. Wu, C. Li, K. Zou, J.Y. Lu. *J. Coord. Chem.*, **64**, 2329 (2011).

[18] J. Wang, X. Qian, Y.-F. Cui, B.-L. Li, H.-Y. Li. *J. Coord. Chem.*, **64**, 2878 (2011).

[19] J. Yang, G.D. Li, J.J. Cao, Q. Yue, G.H. Li, J.S. Chen. *Chem. Eur. J.*, **13**, 3248 (2007).

[20] J. He, J. Yu, Y. Zhang, Q. Pan, Q.R. Xu. *Inorg. Chem.*, **44**, 9279 (2005).